SOILS AND FOUNDATIONS Vol. 26, No. 3, 81-98, Sept. 1986
Japanese Society of Soil Mechanics and Foundation Engineering

A GENERALIZED ELASTOPLASTIC CONSTITUTIVE MODEL FOR CLAY IN THREE-DIMENSIONAL STRESSES

TERUO NAKAI* and HAJIME MATSUOKA*

ABSTRACT

A simple and general elastoplastic constitutive model for clay is proposed that describes the stress-strain behavior of clay under various stress paths in three-dimensional stresses. This model takes into account precisely not only the influence of the intermediate principal stress on the strength and deformation characteristics of clay but also the influence of the stress path on the deformation characteristics of clay. The former influence is considered by using the mechanical quantity t_{ij} which is a generalized idea of the extended concept of "Spatially Mobilized Plane" (briefly SMP*), and the latter influence by dividing the plastic strain increment into two components regardless that only a yield function and a strain hardening parameter are employed. Furthermore, the soil parameters of the proposed model are easily determined in the same manner as the well-known Cam-clay model.

The validities of the proposed model are checked by analyzing various element tests on clay under triaxial compression, triaxial extension and plane strain conditions and comparing these analytical results with the experimental results.

Key words : cohesive soil, constitutive equation of soil, dilatancy, laboratory test, shear strength, static, stress path, stress-strain curve (**IGC** : D 6)

INTRODUCTION

When we apply a constitutive model for soil to the deformation analysis of soil foundations and earth structures, it is necessary for the model to describe uniquely the stress-strain behavior of soil under various three-dimensional stress paths. However, since it is very difficult to express the mechanical behavior of soil in general stress system directly, we usually consider separately the influence of the intermediate principal stress on soil behavior (e. g. differences of deformation and strength characteristics of soils under triaxial compression, triaxial extension and plane strain conditions) and the influence of the stress path on soil behavior (e. g. differences of deformation characteristics of soil under constant minor principal stress path, constant major principal stress path, constant mean principal stress path and constant stress ratio path). For taking into consideration the influence of the intermediate principal stress in elastoplastic constitutive models for

* Associate Professor, Department of Civil Engineering, Nagoya Institute of Technology, Gokiso-cho, Showa-ku, Nagoya.
Manuscript was received for review on December 20, 1985.
Written discussions on this paper should be submitted before April 1, 1987, to the Japanese Society of Soil Mechanics and Foundation Engineering, Sugayama Bldg. 4 F, Kanda Awaji-cho 2-23, Chiyoda-ku, Tokyo 101, Japan. Upon request the closing date may be extended one month.

clay, e. g. Roscoe and Burland (1968) modified a strength parameter in the model so as to satisfy Mohr-Coulomb's criterion, and Lade (1979) introduced a stress ratio parameter J_1^3/J_3(J_1, J_3=first and third effective stress invariants). For taking into consideration the influence of the stress path, Pender (1977) and Ohmaki (1979) proposed double hardening models which contain two sets of yield functions and plastic potential functions (usually, one is for shear and the other for consolidation).

The authors developed a constitutive model in which the influence of the intermediate principal stress is considered by using the extended concept of the "Spatially Mobilized Plane" (briefly SMP*), and the influence of the stress path by dividing the strain increment into the shear component due to the change in stress ratio and the consolidation component due to the change in mean principal stress (Nakai and Matsuoka, 1981, 1983 b). Then, this model were applied to the finite element analyses of soil foundations (Nakai et al., 1982 ; Nakai and Matsuoka, 1983 b ; Nakai, 1985). However, constant mean principal stress tests and a consolidation test should be performed to determine precisely its soil parameters (λ^*, μ^*, μ'^*, γ_{0i}^*, C_d^*, C_c, C_s, K_0 and ϕ'). On the other hand, the well-known Cam-clay model (Roscoe, Schofield and Thurairajah, 1963 ; Schofield and Wroth, 1968) can not describe adequately the influence of the intermediate principal stress and the influerce of the stress path, though its soil parameters (C_c, C_s and ϕ') are easily determined.

In the present study, a simple and general elastoplastic constitutive model for clay, which is named the t_{ij}-clay model, is presented by making use of the basic idea of the above-mentioned constitutive model based on the concept of SMP* while incorporating the merit of the Cam-clay model. That is to say, the influence of intermediate principal stress is considered in this constitutive model by using a mechanical quantity t_{ij} which is a generalized idea of the concept of SMP*. Furthermore, the influence of the stress path is considered even though its foundamental soil parameter are the same as those of the Cam-clay model. This is because the plastic strain increment is divided into the component satisfying the associated flow rule and the other component, though only a yield function and a hardening parameter are used in the model. After describing the contents of the proposed model, the validities of the model are confirmed by the various element tests under triaxial compression and extention conditions and others.

Throughout this paper, the term "stress" is to be interpreted as "effective stress".

OUTLINE OF MECHANICAL QUANTITY t_{ij}

Since the details of the mechanical quantity t_{ij} were described in the former paper (Nakai and Mihara, 1984), only the brief explanation of t_{ij} is shown here.

Fig. 1 shows a cubical soil element and the "Spatially Mobilized Plane(SMP)" in a three-dimensional space, where I, II and III axes represent the direction to which three principal stresses σ_1, σ_2 and σ_3 are applied, respectively. The SMP is indicated by the plane ABC, and the values at the points(A, B and C) where the SMP intersects these three axes

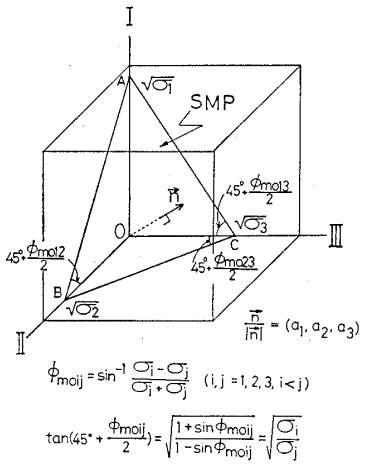

Fig. 1. A cubical soil element and Spatially Mobilized Plane(plane ABC)in three-dimensional space

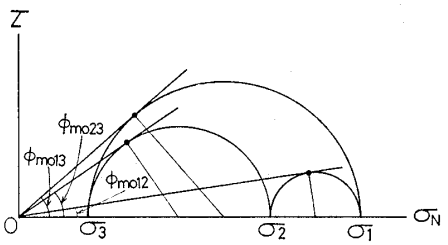

Fig. 2. Explanation of mobilized angles ϕ_{moij} $(i, j=1, 2, 3\ ;\ i<j)$

are proportional to the roots of the respective principal stresses as seen from the equations insetted in Fig. 1 (Matsuoka and Nakai, 1974, 1977). Here, the angles $\phi_{moij}(i, j=1, 2, 3\ ;\ i<j)$ represent the mobilized angles between respective two principal stresses (see Fig. 2). Therefore, the direction cosines(a_1, a_2 and a_3) of the normal to the SMP are expressed as

$$a_i=\sqrt{\frac{J_3}{\sigma_i J_2}} \quad (i=1, 2, 3) \qquad (1)$$

where J_1, J_2 and J_3 are the first, second and third effective stress invariants and expressed by the following forms by the use of the three principal stresses.

$$\left.\begin{aligned} J_1&=\sigma_1+\sigma_2+\sigma_3 \\ J_2&=\sigma_1\sigma_2+\sigma_2\sigma_3+\sigma_3\sigma_1 \\ J_3&=\sigma_1\sigma_2\sigma_3 \end{aligned}\right\} \qquad (2)$$

The mechanical quantity t_{ij} is a symmetrical tensor whose each principal value (t_1, t_2 and t_3) is the product of the corresponding principal stress and the corresponding direction consine of the SMP as follows :

$$\left.\begin{aligned} t_1&=a_1\sigma_1 \\ t_2&=a_2\sigma_2 \\ t_3&=a_3\sigma_3 \end{aligned}\right\} \qquad (3)$$

The tensor t_{ij} can also be expressed as

$$t_{ij}=a_{ik}\cdot\sigma_{kj} \qquad (4)$$

where σ_{kj} is the stress tensor, and a_{ik} is the tensor whose principal values are given by the direction cosines(a_1, a_2 and a_3) of the SMP in Eq. (1). Here, since the principal values $a_i(i=1, 2$ and $3)$ are the function of stress ratio as seen from Eq. (1), the tensor t_{ij} given by Eq. (4) is considered to be a "stress tensor" reflecting the induced anisotropy of such a granular materials as soils

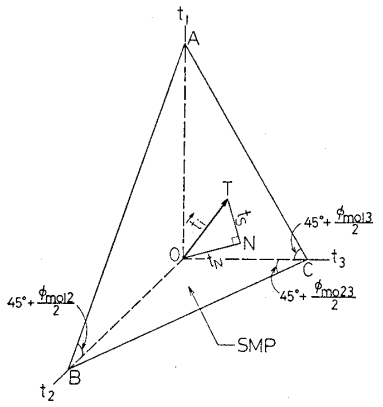

Fig. 3. Stress parameters (t_N and t_S) represented in principal value space of t_{ij}

caused by the change in stress ratio(Nakai and Mihara, 1984).

The stress parameters(t_N and t_S) used in the constitutive model based on the t_{ij} concept are defined as the normal component $\overline{ON}$ and the parallel component $\overline{NT}$ of the principal value vector of t_{ij}, $\overrightarrow{OT}=\vec{t_i}=(t_1, t_2, t_3)$, to the SMP as shown in Fig. 3, and are also equivalent to the normal and shear stresses (σ_{SMP} and τ_{SMP}) on the SMP, respectively.

$$t_N=t_1a_1+t_2a_2+t_3a_3 \qquad (5)_1$$

$$\left(\equiv\sigma_{SMP}=\sigma_1a_1^2+\sigma_2a_2^2+\sigma_2a_2^2=3\frac{J_3}{J_2}\right) \qquad (5)_2$$

$$t_S=\sqrt{(t_1a_2-t_2a_1)^2+(t_2a_3-t_3a_2)^2+(t_3a_1-t_1a_3)^2} \qquad (6)_1$$

$$\left(\equiv\tau_{SMP}=\sqrt{\begin{aligned}&(\sigma_1-\sigma_2)^2a_1^2a_2^2\\&+(\sigma_2-\sigma_3)^2a_2^2a_3^2+(\sigma_3-\sigma_1)^2a_3^2a_1^2\end{aligned}}=\sqrt{\frac{J_1J_2J_3-9J_3^2}{J_2}}\right) \qquad (6)_2$$

From Eqs. $(5)_2$ and $(6)_2$, the stress ratio, $X\equiv t_S/t_N$, are also given by

$$X\equiv\frac{t_S}{t_N}=\sqrt{\frac{J_1J_2-9J_3}{9J_3}} \qquad (7)$$

For reference, the stress parameters(p and q) which are often used in many constitutive models such as the Cam-clay model are expressed as

$$p=\sigma_m=\frac{1}{3}(\sigma_1+\sigma_2+\sigma_3) \qquad (8)$$

$$q=\frac{1}{\sqrt{2}}\sqrt{(\sigma_1-\sigma_2)^2+(\sigma_2-\sigma_3)^2+(\sigma_3-\sigma_1)^2} \qquad (9)$$

Now, when we develop an elastoplastic constitutive model of soil, we usually consider the yield function and/or the plastic potential function by the use of the stress parameters (p and q) of Eqs. (8) and (9) and assume the flow rule in a space of stress, σ_{ij}. However, such a constitutive model can not describe the stress-strain behavior of soil under three different principal stresses by the same values of soil parameters, as seen from e. g. Cam-clay model. Frankly speaking about a merit of introducing the proposed t_{ij} concept, it becomes possible to describe uniquely the soil behavior in three-dimensional stresses by specifying the yield function and/or the plastic potential function using the stress parameters(t_N and t_S) instead of (p and q) together with the flow rule in the t_{ij}-space instead of the σ_{ij}-space (Nakai and Mihara, 1984).

ELASTOPLASTIC CONSTITUTIVE MODEL FOR CLAY

As shown in Eq. (10), it is assumed that the plastic strain increment tensor, $d\varepsilon_{ij}^p$, is divided into two components ; the component which satisfies the associated flow rule in the t_{ij}-space, $d\varepsilon_{ij}^{p(AF)}$, and the component compressive isotropically, $d\varepsilon_{ij}^{p(IC)}$

$$d\varepsilon_{ij}^p = d\varepsilon_{ij}^{p(AF)} + d\varepsilon_{ij}^{p(IC)} \tag{10}$$

These two plastic strain increment tensors, $d\varepsilon_{ij}^{p(AF)}$ and $d\varepsilon_{ij}^{p(IC)}$, are given as follows, since the direction of $d\varepsilon_{ij}^{p(AF)}$ is normal to the yield surface f in the t_{ij}-space, and $d\varepsilon_{ij}^{p(IC)}$ is the isotropic compression component :

$$d\varepsilon_{ij}^{p(AF)} = \Lambda \cdot \frac{\partial f}{\partial t_{ij}} \tag{11}$$

$$d\varepsilon_{ij}^{p(IC)} = \frac{\delta_{ij}}{3} \cdot K \cdot \langle dt_N \rangle \tag{12}$$

Here, δ_{ij} is the Kronecker delta, and $\langle dt_N \rangle$ indicates that

$$\langle dt_N \rangle = \begin{cases} dt_N & \text{if } dt_N > 0 \\ 0 & \text{if } dt_N \leqq 0 \end{cases} \tag{13}$$

In the present paper, superscripts e, p, (AF) and (IC) denote the elastic component, the plastic component, the component satisfying the associated flow rule and the component compressive isotropically, respectively.

The way to determine the yield function f, the proportionality constant Λ and the coefficient of isotropic compression component K will be discussed next.

1) Determination of yield function f

In the Cam-clay model, the yield function (plastic potential function) of the original model is determined from the normality condition and the following stress ratio-plastic strain increment ratio relation :

$$\frac{d\varepsilon_v^p}{d\varepsilon_d^p} = M - \frac{q}{p} \quad (M = q/p \text{ at citical state}) \tag{14}$$

using the stress parameters given by Eqs. (8) and (9) and the plastic strain increment parameters given by

$$d\varepsilon_v^p = d\varepsilon_1^p + d\varepsilon_2^p + d\varepsilon_3^p \tag{15}$$

$$d\varepsilon_d^p = \frac{\sqrt{2}}{3}\sqrt{(d\varepsilon_1^p - d\varepsilon_2^p)^2 + (d\varepsilon_2^p - d\varepsilon_3^p)^2 + (d\varepsilon_3^p - d\varepsilon_1^p)^2} \tag{16}$$

It has, however, been shown by test results on clay and sand that such a equation as Eq. (14) using the stress and plastic strain increment parameters of Eqs. (8), (9), (15) and (16) does not describe the stress-dilatancy behavior of soils in three-dimensional stresses universally(e. g. Nakai and Matsuoka, 1983a; Nakai et al., 1986).

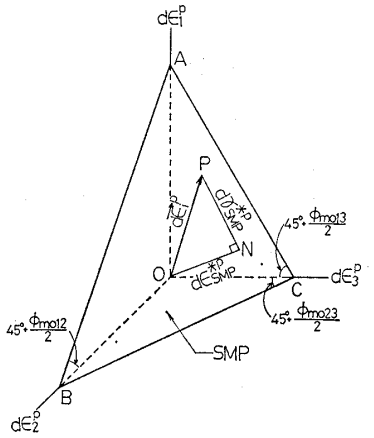

Fig. 4. Plastic strain increment parameters ($d\varepsilon_{SMP}{}^{*p}$ and $d\gamma_{SMP}{}^{*p}$) represented in plastic principal strain increment space

On the other hand, according to the extended concept of the "Spatially Mobilized Plane" (SMP* concept) from which the quantity t_{ij} is derived, various shear test results under three different principal stresses can be uniquely arranged in terms of the relation between the stress ratio $X \equiv t_S/t_N \equiv \tau_{SMP}/\sigma_{SMP}$ and the strain increment ratio $d\varepsilon_{SMP}{}^{*p}/d\gamma_{SMP}{}^{*p}$ (Nakai and Matsuoka, 1980, 1983 a). Here, the stresses $t_N \equiv \sigma_{SMP}$ and $t_S \equiv \tau_{SMP}$ are given by Eqs. (5) and (6), and the strain increments $d\varepsilon_{SMP}{}^{*p}$ and $d\gamma_{SMP}{}^{*p}$ are the normal and parallel components of the plastic principal strain increment vector, $\overrightarrow{d\varepsilon_i{}^p} = (d\varepsilon_1{}^p, d\varepsilon_2{}^p, d\varepsilon_3{}^p)$, to the SMP respectively (see Fig. 4) and are expressed as follows :

$$d\varepsilon_{SMP}{}^{*p} = d\varepsilon_1{}^p a_1 + d\varepsilon_2{}^p a_2 + d\varepsilon_3{}^p a_3 \tag{17}$$

$$d\gamma_{SMP}{}^{*p} = \sqrt{\begin{array}{l}(d\varepsilon_1{}^p a_2 - d\varepsilon_2{}^p a_1)^2 \\ +(d\varepsilon_2{}^p a_3 - d\varepsilon_3{}^p a_2)^2 + (d\varepsilon_3{}^p a_1 - d\varepsilon_1{}^p a_3)^2\end{array}} \tag{18}$$

Therefore, in the present study, to determine a yield function the following stress ratio-plastic strain increment ratio relation is assumed, because only the component $d\varepsilon_{ij}{}^{p(AF)}$ satisfies the associated flow rule :

$$Y = \frac{X_f - X}{\alpha} + Y_f \tag{19}$$

in which

$$X \equiv t_S/t_N \text{ and } Y \equiv d\varepsilon_{SMP}{}^{*p(AF)}/d\gamma_{SMP}{}^{*p(AF)}$$

In Eq. (19), X_f and Y_f represent the stress ratio at failure, $(t_S/t_N)_f$, and the plastic strain increment ratio at failure, $(d\varepsilon_{SMP}{}^{*p(AF)}/d\gamma_{SMP}{}^{*p(AF)})_f$. Now, we assume that the critical state condition in three-dimensional stresses is determined by the following Matsuoka-Nakai failure criterion (SMP failure criterion) (Matsuoka and Nakai, 1974, 1977).

$$X_f \equiv \left(\frac{t_S}{t_N}\right)_f \equiv \left(\frac{\tau_{SMP}}{\sigma_{SMP}}\right)_f = \text{const.} \tag{20}$$

or

$$\frac{J_1 J_2}{J_3} = \text{const.} \tag{21}$$

Then, if it is assumed that at any critical state condition under a triaxial compression ($\sigma_1 > \sigma_2 = \sigma_3$) a soil element undergoing shear distortion deforms without further change in plastic volumetric strain, the stress ratio X_f and plastic strain increment ratio Y_f at failure, i. e. at the critical state, are expressed as follows by the major-minor principal stress ratio at failure under triaxial compression, R_f : (see Appendix 1)

$$X_f = \frac{\sqrt{2}}{3}\left(\sqrt{R_f} - \sqrt{\frac{1}{R_f}}\right) \tag{22}$$

$$Y_f = \frac{1-\sqrt{R_f}}{\sqrt{2}\,(\sqrt{R_f}+0.5)} \tag{23}$$

where

$$R_f \equiv \left(\frac{\sigma_1}{\sigma_3}\right)_{f\,(\text{comp.})} = \frac{1+\sin\phi'_{(\text{comp.})}}{1-\sin\phi'_{(\text{comp.})}} \tag{24}$$

Throughout this paper, subscripts f, (comp.) and (ext.) denote the values at failure condition, at triaxial compression condition and at triaxial extension condition, respectively.

Fig. 5 shows the stress ratio-plastic strain increment ratio relationship of Eq. (19), where $X_f = 0.63$, $Y_f = -0.26$ and $\alpha = 0.7$ are the values determined for the Fujinomori clay which will be described later. As seen from this figure, the parameter α denotes the linear gradient of the line, and the ordinate intercept M^* is expressed as

$$M^* = X_f + \alpha \cdot Y_f \tag{25}$$

If it is assumed that the directions of the principal axes of t_{ij} coincide with those of the plastic principal strain increments and that the associated flow rule holds in the t_{ij}-

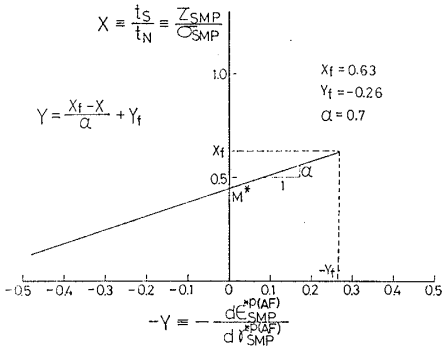

Fig. 5. Proposed relation between stress ratio (t_S/t_N) and plastic strain increment ratio ($-d\varepsilon_{SMP}{}^{*p(AF)}/d\gamma_{SMP}{}^{*p(AF)}$)

space, the following normality condition is obtained.

$$dt_1\cdot d\varepsilon_1{}^{p(AF)}+dt_2\cdot d\varepsilon_2{}^{p(AF)}+dt_3\cdot d\varepsilon_3{}^{p(AF)} =dt_N\cdot d\varepsilon_{SMP}{}^{*p(AF)}+dt_S\cdot d\gamma_{SMP}{}^{*p(AF)} =0 \quad (26)$$

Solving the differential equation which is derived by combining Eqs. (19) and (26), we can obtain

$$\ln t_N+\frac{-\alpha}{1-\alpha}\ln\left|1-(1-\alpha)\frac{X}{M^*}\right| -\ln t_{N1}=0 \quad (\alpha\neq 1) \quad (27\,a)$$

$$\ln t_N+\frac{X}{M^*}-\ln t_{N1}=0 \quad (\alpha=1) \quad (27\,b)$$

where M^* is given by Eq. (25), and t_{N1} is the value of t_N at $t_S=0$.

Now, we regard the plastic volumetric strain $\varepsilon_v{}^p$ as the strain hardening parameter and assumed that $\varepsilon_v{}^p$ can be given by the following equation under a constant stress ratio condition (e. g. isotropic consolidation and K_0-consolidation) in the same manner as the Cam-clay model.

$$\varepsilon_v{}^p=\frac{\lambda-\kappa}{1+e_0}\ln\frac{t_N}{t_{N0}}\left(=\frac{\lambda-\kappa}{1+e_0}\ln\frac{p}{p_0}\right) \quad (28)$$

Here, p is the effective mean principal stress, e_0 is the intial void ratio at $t_S=0$ and $t_N=t_{N0}(=p_0)$, λ is the compression index$(=0.434\,C_c)$ and κ is the swelling index$(=0.434\,C_s)$. Therefore, from Eqs. (27) and (28), we can eventually obtain the following yield function.

$$f=\frac{\lambda-\kappa}{1+e_0}\left[\ln\frac{t_N}{t_{N0}}+\frac{-\alpha}{1-\alpha}\ln\left|1-(1-\alpha)\frac{X}{M^*}\right|\right] -\varepsilon_v{}^p=0 \quad (\alpha\neq 1) \quad (29\,a)$$

$$f=\frac{\lambda-\kappa}{1+e_0}\left[\ln\frac{t_N}{t_{N0}}+\frac{X}{M^*}\right]-\varepsilon_v{}^p=0 \quad (\alpha=1) \quad (29\,b)$$

Here, the yield function at $\alpha=1$, Eq. (29 b), is the same as that in the previous paper (Nakai and Mihara, 1984), which is derived by applying the quantity t_{ij} to the original Cam-clay model (Schofield and Wroth, 1968) or Ohta's model (Ohta, 1971).

2) *Determination of* $d\varepsilon_{ij}{}^{p(AF)}$

If the yield function f mentioned above is given, the plastic strain increment which satisfies the associated flow rule, $d\varepsilon_{ij}{}^{p(AF)}$, is calculated by using Eq. (11). We will herein mention how to determine the proportionality constant Λ in Eq. (11), which represents the magnitude of strain hardening.

Since the yield function f is given in the form of $f=f(t_{ij},\ a_i,\ \varepsilon_v{}^p)=f(\sigma_{ij},\ \varepsilon_v{}^p)=0$, the condition of consistency is expressed as

$$df=\frac{\partial f}{\partial\sigma_{ij}}d\sigma_{ij}+\frac{\partial f}{\partial\varepsilon_v{}^p}\cdot\frac{\partial\varepsilon_v{}^p}{\partial\varepsilon_{kl}{}^p}d\varepsilon_{kl}{}^p=0 \quad (30)$$

Here, from Eqs. (10), (11) and (12), $d\varepsilon_{ij}{}^p$ is given by

$$d\varepsilon_{ij}{}^p=\Lambda\frac{\partial f}{\partial t_{ij}}+\frac{\delta_{ij}}{3}\cdot K\cdot\langle dt_N\rangle \quad (31)$$

so that by combining Eqs. (30) and (31), the proportionality constant Λ is expressed as

$$\Lambda=-\frac{\dfrac{\partial f}{\partial\sigma_{ij}}d\sigma_{ij}+\dfrac{\partial f}{\partial\varepsilon_v{}^p}\cdot\dfrac{\partial\varepsilon_v{}^p}{\partial\varepsilon_{mn}{}^p}\cdot\dfrac{\delta_{mn}}{3}\cdot K\cdot\langle dt_N\rangle}{\dfrac{\partial f}{\partial\varepsilon_v{}^p}\cdot\dfrac{\partial\varepsilon_v{}^p}{\partial\varepsilon_{kl}{}^p}\cdot\dfrac{\partial f}{\partial t_{kl}}} =\frac{\dfrac{\partial f}{\partial\sigma_{ij}}d\sigma_{ij}-K\cdot\langle dt_N\rangle}{\dfrac{\partial f}{\partial t_{kk}}} \quad (32)$$

See Appendix 2 about the concrete forms of the derivatives $\partial f/\partial t_{ij}$, $\partial f/\partial\varepsilon_v{}^p$, $\partial\varepsilon_v{}^p/\partial\varepsilon_{ij}{}^p$ and $\partial f/\partial\sigma_{ij}$.

3) *Determination of* $d\varepsilon_{ij}{}^{p(IC)}$

Under a constant stress ratio, the plastic volumetric strain increment $d\varepsilon_v{}^p$ are given by the following equation from Eq. (28).

$$d\varepsilon_v{}^p=\frac{\lambda-\kappa}{1+e_0}\cdot\frac{\langle dp\rangle}{p}=\frac{\lambda-\kappa}{1+e_0}\cdot\frac{\langle dt_N\rangle}{t_N} \quad (33)$$

(since $dp/p=dt_N/t_N$ when stress ratio is constant)

Now, the current stress condition is considered to be at point A on the yield surface f in Fig. 6. It is then assumed that the plastic volumetric strain increment compressive isotropically $d\varepsilon_v{}^{p(IC)}$ is t_N/t_{N1} of the plastic volumetric strain increment $d\varepsilon_v{}^p$ given by Eq. (33)

$$d\varepsilon_v{}^{p(IC)}=\frac{\lambda-\kappa}{1+e_0}\cdot\frac{\langle dt_N\rangle}{t_N}\cdot\frac{t_N}{t_{N1}} \quad (34)$$

where t_{N1} is the value of the intersection of the current yield surface with the t_N-axis (point P in Fig. 6). By evaluating $d\varepsilon_v{}^{p(IC)}$ in such a way, for example, under a constant

stress ratio the ratio $d\varepsilon_v{}^{p(IC)} : d\varepsilon_v{}^{p(AF)}$ is expressed as $t_N/t_{N1} : (1-t_N/t_{N1})$, and the relative proportion of $d\varepsilon_v{}^{p(IC)}$ decreases with increase in the stress ratio. As the result, we can describe properly the stress-strain behavior of clay under various constant stress ratios that though there is a unique linear relation between ε_v and ln p (ln t_N), the shear strain becomes large as the stress ratio increases.

From Eq. (34), we give the plastic strain increment compressive isotropically, $d\varepsilon_{ij}{}^{p(IC)}$, under the general stress condition in the forms of

$$d\varepsilon_{ij}{}^{p(IC)} = \frac{\delta_{ij}}{3}\cdot\frac{\lambda-\kappa}{1+e_0}\cdot\frac{\langle dt_N\rangle}{t_N}\cdot\frac{t_N}{t_{N1}} = \frac{\delta_{ij}}{3}\cdot K\cdot\langle dt_N\rangle \qquad (35)$$

so that the coefficient K is

$$K = \frac{\lambda-\kappa}{1+e_0}\cdot\frac{1}{t_N}\cdot\frac{t_N}{t_{N1}} \qquad (36)$$

The ratio t_N/t_{N1} is expressed by the following equation from Eq. (27)

$$\frac{t_N}{t_{N1}} = \left|1-(1-\alpha)\frac{X}{M^*}\right|^{\alpha/(1-\alpha)} \qquad (\alpha\neq 1) \qquad (37\,a)$$

$$\frac{t_N}{t_{N1}} = \exp\left(\frac{-X}{M^*}\right) \qquad (\alpha=1) \qquad (37\,b)$$

Here, since the stress parameter t_N is given by Eq. $(5)_2$, the increment dt_N is expressed as follows by use of stress increment tensor $d\sigma_{ij}$

$$dt_N = \frac{\partial t_N}{\partial\sigma_{ij}}d\sigma_{ij} = \frac{\partial\left(3\dfrac{J_3}{J_2}\right)}{\partial\sigma_{ij}}d\sigma_{ij} \qquad (38)$$

4) *Complete form of the constitutive model*

The elastic strain increment tensor $d\varepsilon_{ij}{}^e$ is given by use of generalized Hooke's law.

$$d\varepsilon_{ij}{}^e = \frac{1+\nu_e}{E_e}d\sigma_{ij} - \frac{\nu_e}{E_e}d\sigma_{kk}\cdot\delta_{ij} \qquad (39)$$

where Young's modulus E_e is expressed in terms of the swelling index κ and Poisson's ratio ν_e as

$$E_e = \frac{3(1-2\nu_e)(1+e_0)p}{\kappa} \qquad (40)$$

Therefore, the total strain increment tensor $d\varepsilon_{ij}$ is given by the following form as the summation of $d\varepsilon_{ij}{}^p$ in Eqs. (10) to (12) and $d\varepsilon_{ij}{}^e$ in Eq. (39).

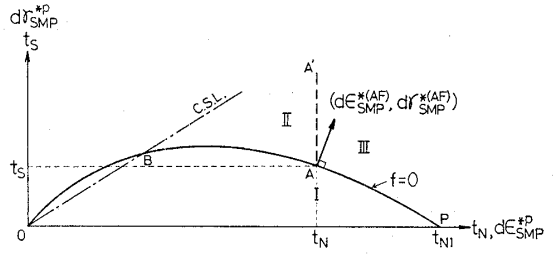

Fig. 6. Proposed yield surface f represented in (t_N, t_S) space and direction of plastic strain increment which satisfies associated flow rule in t_{ij}-space

$$d\varepsilon_{ij} = d\varepsilon_{ij}{}^p + d\varepsilon_{ij}{}^e = d\varepsilon_{ij}{}^{p(AF)} + d\varepsilon_{ij}{}^{p(IC)} + d\varepsilon_{ij}{}^e \qquad (41)$$

5) *Characteristics of the constitutive model*

Firstly, let us explain the development of strain under various stress paths by using Fig. 6. Fig. 6 shows the direction of plastic strain increment which satisfies the associated flow rule by a vector in the $(d\varepsilon_{SMP}{}^{*p}, d\gamma_{SMP}{}^{*p})$ space, together with the yield surface f in the (t_N, t_S) space.

(i) If the stress condition lies inside the current yield surface or moves from point A to region I(f<0 or $df\leqq 0$) :

$$d\varepsilon_{ij} = d\varepsilon_{ij}{}^e \qquad (42)$$

(ii) If the stress condition moves from point A to region II($f=0$, $df>0$ and $dt_N\leqq 0$) :

$$d\varepsilon_{ij} = d\varepsilon_{ij}{}^{p(AF)} + d\varepsilon_{ij}{}^e \qquad (43)$$

(since $d\varepsilon_{ij}{}^p = d\varepsilon_{ij}{}^{p(AF)}$ when $dt_N\leqq 0$)

(iii) If the stress condition moves from point A to region III($f=0$, $df>0$ and $dt_N>0$) :

$$d\varepsilon_{ij} = d\varepsilon_{ij}{}^{p(AF)} + d\varepsilon_{ij}{}^{p(IC)} + d\varepsilon_{ij}{}^e \qquad (44)$$

Dividing the plastic strain increment into two components at region III in such a way, we can describe the stress path dependency of the direction of plastic strain increment.

Now then, though the proportionality constant A of Eq. (32) is usually positive under the stress paths such as σ_m=const., σ_1=const., σ_3=const. and $R\equiv\sigma_1/\sigma_3$=const., there happens that A becomes negative according

to the stress path. We will show in Appendix 3 how to formulate the model in such a case.

Fig. 7 shows the yield surface of the proposed model for the Fujinomori clay in the (p, q) space, in the same fashion to specify the Cam-clay model. The upper half indicates the one in triaxial compression, and the lower half the one in triaxial extension. The yield surface is not symmetric with respect to the p-axis, though the yield surface of the Cam-clay model is symmetric. Although the vectors in this figure indicate the directions of the plastic strain increment vectors satisfying the associated flow rule,

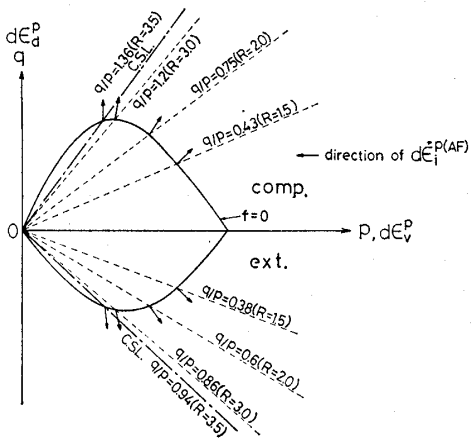

Fig. 7. Proposed yield surface f represented in (p, q) space and directions of plastic strain increment which satisfies associated flow rule in t_{ij}-space

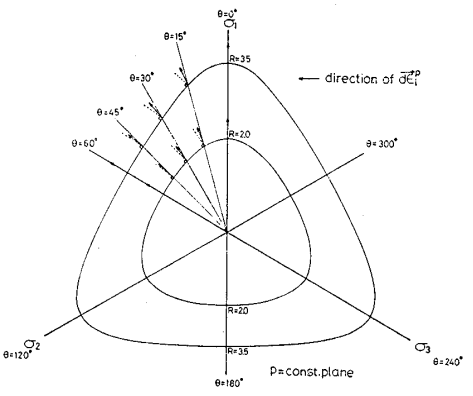

Fig. 8. Proposed yield surface represented on octahedral plane and directions of plastic strain increment

$\overrightarrow{d\varepsilon_i^{p(AF)}}$, it should be noticed that the vectors are not normal to the yield surface. This is because in the present model the associated flow rule holds not in the stress space such as (p, q) but in the t_{ij}-space.

Fig. 8 shows the yield surface on the octahedral plane in the principal stress space for two cases of $R \equiv (\sigma_1/\sigma_3)_{(\text{comp.})} \equiv (\sigma_1/\sigma_3)_{(\text{ext.})} = 2$ and 3.5. The shape of the yield surface on the octahedral plane is in agreement with the Matsuoka-Nakai criterion (SMP criterion) represented by Eq. (20) or (21). In this figure, the vectors indicate the directions of the plastic strain increment vectors $\overrightarrow{d\varepsilon_i^p}$ on the octahedral plane, i. e., direction of $\overrightarrow{d\varepsilon_d^p}$, under the stress conditions of $\theta = 0°$, 15°, 30°, 45° and 60°, where θ denotes the angle from the σ_1-axis on the octahedral plane. Since the parallel component of $\overrightarrow{d\varepsilon_i^{p(IC)}}$ to the octahedral plane is always zero, the direction of $\overrightarrow{d\varepsilon_d^p}$ coincides with that of $\overrightarrow{d\varepsilon_d^{p(AF)}}$. As is seen from this figure, under the three different principal stresses ($\theta = 15°$, 30°, 45°) the direction of each vector deviates from that of the corresponding deviatoric stress vector, i. e. radial direction, with a definite trend as the stress ratio increases. It is also noticed that its direction is not normal to the yield surface in the same manner as Fig. 7 and is between the radial direction and the direction normal to the yield surface (direction of broken lines). This tendency predicted by the proposed model corresponds to that of many true triaxial test results on clay (e. g. Youg and Mckyes, 1971 ; Lade and Musante, 1978 ; Nakai et al., 1986).

METHODS TO DETERMINE SOIL PARAMETERS

The fundamental soil parameters of the proposed model are the same as those of the Cam-clay model (λ, κ and $\phi'_{(\text{comp.})}$) plus a parameter which is the linear gradient α in Fig. 5. Since the parameters λ, κ and $\phi'_{(\text{comp.})}$ are determined from the e-ln p relationship in a consolidation test and the strength of a conventional triaxial compres-

sion test, in the same manner as the Cam-clay model, we will discuss the method to determine the parameter α.

(1) Method to determine from undrained test

The elastic volumetric strain $\varepsilon_v{}^e$ is given by

$$\varepsilon_v{}^e=\frac{\kappa}{1+e_0}\ln\left(\frac{p}{p_0}\right) \tag{45}$$

and the plastic volumetric strain is given by Eq. (29). Here, by considering the undrained condition ($\varepsilon_v=\varepsilon_v{}^e+\varepsilon_v{}^p=0$), the ratio of the mean principal stress at criterial state, p_c, to that at initial isotropic condition, p_0, (see Fig. 9) in undrained triaxial test is expresses as follows :

$$\frac{p_c}{p_0}=\left[(X_f{}^2+1)\cdot\left|1-(1-\alpha)\frac{X_f}{M^*}\right|^{\alpha/(1-\alpha)}\right]^{(1-(\kappa/\lambda))} \tag{46}$$

where on obtaining this form, the following relation is used,

$$p=t_N\cdot(X^2+1) \tag{47}$$

Fig. 10 shows the relationship between p_c/p_0 and ϕ' obtained from Eq. (46) for various values of κ/λ and α. Here, analytical results by the original and modified Cam-clay models are also drawn with the broken lines and the dash-dotted lines, respectively. Thus, we can estimate the value of α with reference to Eq. (46) and/or Fig. 10.

(2) Method to determine from K_0-value

Fig. 11 shows the predicted variations of K_0-value in terms of the relation between K_0 and ϕ' for various values of α and κ/λ. In calculation the Poisson ratio ν_e is assumed to be 0.0, since the elastic shear strain is relatively small. The broken lines in this figure indicate Jaky's empirical expression, $K_0=1-\sin\phi'$. We can therefore estimate α from K_0-value using this figure. On the other hand, if we determine α in other ways,

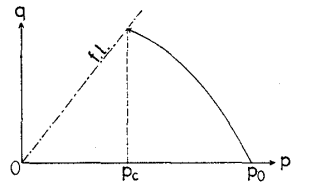

Fig. 9. Explanation of p_c and p_0 in undrained triaxial test

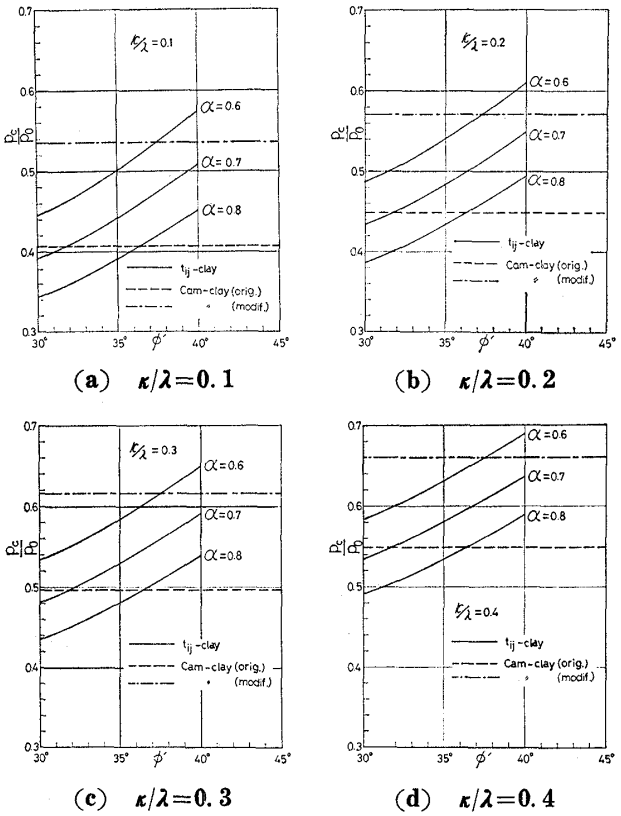

Fig. 10. Analytical relation between ratio p_c/p_0 and internal friction angle ϕ' in undrained triaxial test

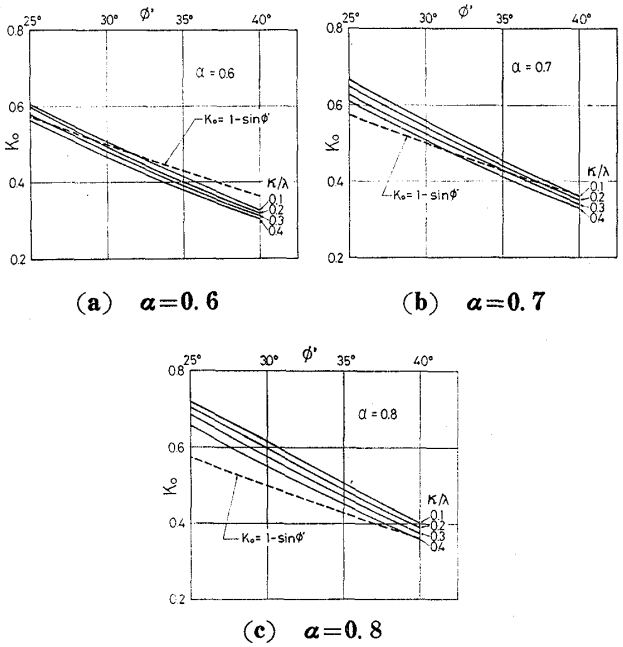

Fig. 11. Analytical relation between K_0-value and internal friction angle ϕ' in K_0-consolidation test

we can predict K_0-value from this figure.

(3) Other methods

As is seen in Figs. 10 and 11, the value of α usually lies between about 0.6 and 0.8. Therefore, when any element test is performed, by assuming the proper value of α and fitting the predicted stress-strain curve to the observed values, the parameter α can be estimated.

VERIFICATION OF PROPOSED MODEL

Saturated remoulded normally consolidated Fujinomori clay (F-clay) was used in the experiments. Physical properties of the Fujinomori clay are as follows : the liquid limit $w_L=44.7\%$, the plastic limit $w_p=24.7\%$ and the specific gravity $G_s=2.65$. The specimens were prepared by one-dimensionally consolidating the clay mixed with deaired water under a pressure of 49 kN/m^2 and forming this consolidated clay in the shape of cylinders of 3.5 cm in diameter and 8 cm in height. The initial water content of the specimens under this condition was approximately 40%. Tests were performed under various stress paths in triaxial compression and extention conditions. In the undrained shear tests, a back pressure of 98 kN/m^2 was applied. All the tests except for an isotropic consolidation test were performed by means of the strain controlled method at a sufficiently low speed of axial strain rate ($\dot{\varepsilon}_a=5.5\times 10^{-6}$/min). Although only the verifications by the triaxial compression and extention tests are shown in the present paper, the verifications by the true triaxial tests are shown in another paper (Nakai et al., 1986).

The values of soil parameters of Fujinomori clay are listed in Table 1. Here, $\lambda/(1+e_0)$ and $\phi'_{(\mathrm{comp.})}$ are determined from a consolidation test and a conventional triaxial compression test, respectively. Since it is difficult to determine the swelling index κ accurately from the unloading and/or reloading e-ln p curve of a consolidation test, $\kappa/(1+e_0)$ is determined from the values of λ and $\phi'_{(\mathrm{comp.})}$ and Karube's empirical relation (Karube, 1975) given by

$$1-\frac{\kappa}{\lambda}=\frac{M}{1.75} \tag{48}$$

where M is q/p at the critical state and is expressed as

$$M=\frac{6\sin\phi'_{(\mathrm{comp.})}}{3-\sin\phi'_{(\mathrm{comp.})}} \tag{49}$$

The Poisson ratio ν_e is assumed to be 0.0, since the elastic shear strain is relatively small. The value of α is determined by considering that the stress-strain curve in undrained triaxial compression test predicted by the proposed model is approximately the same as that predicted by the original Cam-clay model.

Figs. 12 and 13 show the analytical stress-strain curves and the observed values(dots) in the constant mean principal stress tests ($\sigma_m=196$ kN/m^2), the constant minor principal stress tests($\sigma_3=196$ kN/m^2) and the constant major principal stress tests($\sigma_1=196$ kN/m^2) under triaxial compression and extention conditions respectively, in terms of the relation among major-minor principal stress ratio σ_1/σ_3, major principal strain ε_1 and volumetric strain ε_v. Here, the solid curves repre-

Table 1. Values of soil parameters for clay used in analysis

$\lambda/(1+e_0)$	5.08×10^{-2}
$\kappa/(1+e_0)$	1.12×10^{-2}
$\phi'_{(\mathrm{comp.})}$	33.7°
α	0.7
ν_e	0.0

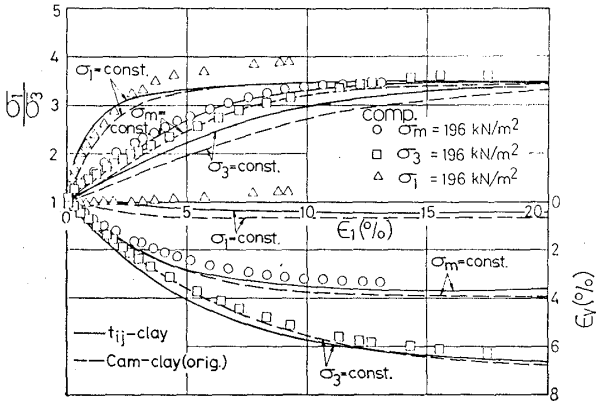

Fig. 12. Major principal strain vs. principal stress ratio and volumetric strain in triaxial compression tests

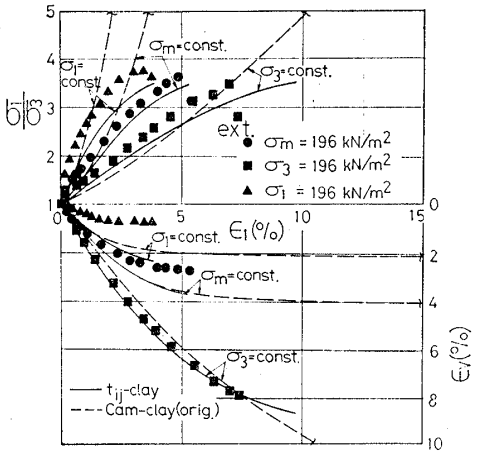

Fig. 13. Major principal strain vs. principal stress ratio and volumetric strain in triaxial extension tests

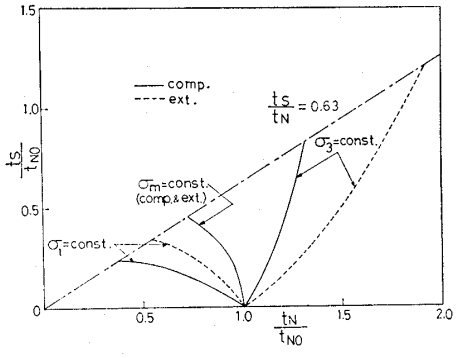

Fig. 14. Stress paths of σ_m=const., σ_1=const. and σ_3=const. tests under triaxial compression and extension conditions represented in (t_N, t_S) space

sent the results calculated by the proposed model(t_{ij}-clay model) and the broken curves that by the original Cam-clay model. In Fig. 14 are drawn the stress paths in these six shear tests, in the space of (t_N, t_S) which are the stress parameters of the t_{ij}-model, where t_{N0} denotes the value of t_N at the initial condition. As is shown in this figure, $dt_N<0$ under the stress conditions of σ_m=const. and σ_1=const., and $dt_N>0$ under the stress conditions of σ_3=const. Therefore, though the plastic strain calculated by the proposed model is all due to the component satisfying the associated flow rule in σ_m=const. and σ_1=const. tests, the plastic strain is given by the summation of the two components(one satifying the associated flow rule and the other compressive isotropically) in σ_3=const. test. It is seen in Fig. 12 that for example ε_1 in σ_3=const. test calculated by the Cam-clay model is larger than that by the proposed model and the observed values. This difference of ε_1 between the two models depends mainly on whether the plastic strain increment is divided into two components, $d\varepsilon_{ij}^{p(AF)}$ and $d\varepsilon_{ij}^{p(IC)}$, or not. In addition, the stress-strain curves by the Cam-clay model in Fig. 13 overestimate the strength of clay. According to the Cam-clay model, the predicted stress ratio at failure in triaxial extension, $(\sigma_1/\sigma_3)_{f(\text{ext.})}$, is 16.0 and is much larger than that under triaxial compression, $(\sigma_1/\sigma_3)_{f(\text{comp.})}=3.5$. This is because the extended Mises failure criterion is used in the Cam-clay model. On the other hand, the values of $(\sigma_1/\sigma_3)_f$ in both triaxial compression and extension predicted by the proposed model are identical and agree with the observed values.

Fig. 15 shows the analytical stress-strain curves under plane strain condition calculated by the two models, and Fig. 16 shows the analytical relation between $b=(\sigma_2-\sigma_3)/(\sigma_1-\sigma_3)$ and σ_1/σ_3 under plane strain condition. Here, the value of b represents the relative magnitude of the intermediate principal stress and is 0.0 for triaxial compression condition and 1.0 for triaxial extension condition. As is seen from these figures, the Cam-clay model gives the excessive strength $((\sigma_1/\sigma_3)_f=$

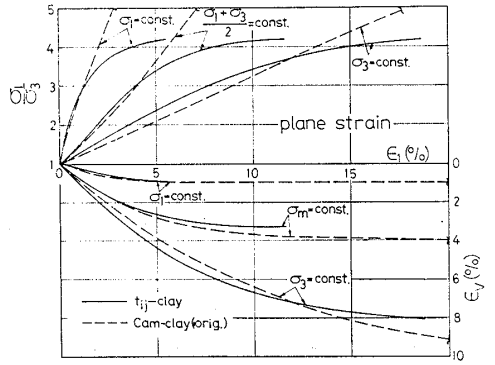

Fig. 15. Calculated major principal strain vs. principal stress ratio and volumetric strain in plane strain tests

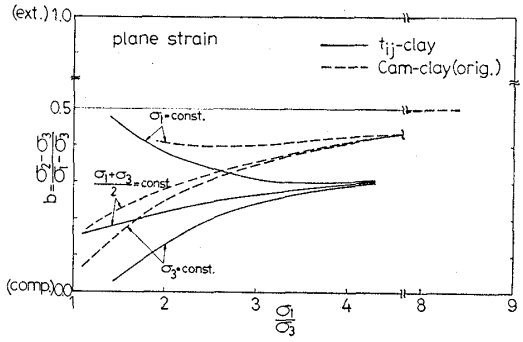

Fig. 16. Calculated variations of b-value in plane strain tests

8. 4) under plane strain condition in the same manner as under triaxial extension condition, and the analytical values of b converge to 0. 5. However, on the basis of the proposed model, the analytical values of $(\sigma_1/\sigma_3)_f$ and b_f under plane strain condition are estimated as $(\sigma_1/\sigma_3)_f=4.24$ and $b_f=0.30\sim0.31$ and correspond to the tendency of many reported experimental results (e. g. Hambly, 1972 ; Vaid and Campanella, 1974). As mentioned above, the strength $(\sigma_1/\sigma_3)_f$ predicted by the proposed model has the same value under triaxial compression and extension conditions and has a little higher value under plane strain condition. This is because we use the Matsuoka-Nakai failure criterion(SMP criterion) in Eq. (20) or (21) whose shape is represented as a curve circumscribing the distorted hexagon of Mohr-Coulomb failure criterion on the octahedral plane in principal stress space as shown in Fig. 8.

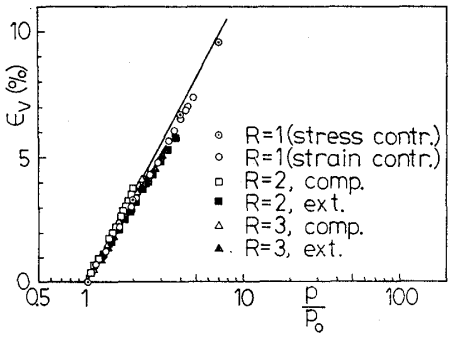

Fig. 17. Mean principal stress vs. volumetric strain in isotropic and anisotropic consolidation tests under triaxial compression and extension conditions

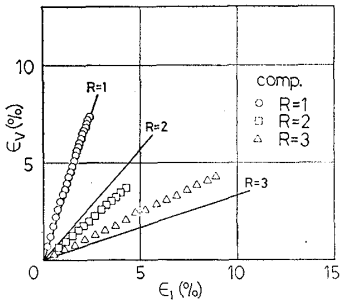

(a) triaxial compression

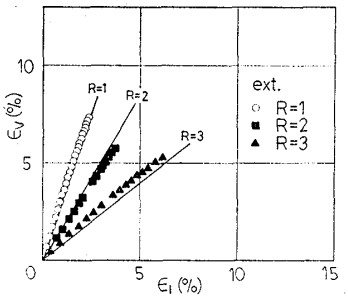

(b) triaxial extension

Fig. 18. Major principal strain vs. volumetric strain in isotropic and anisotropic consolidation tests

Figs. 17 and 18 show the comparisons between the observed values(dots) and the analytical results by the proposed model(solid lines) in the isotropic and anisotropic consolidation tests under triaxial compression and extension conditions, where R denotes the principal stress ratio σ_1/σ_3. Fig. 17 shows the ε_v-$\ln(p/p_0)$ relation(p_0=initial mean principal stress of each consolidation test), and Fig. 18 the $\varepsilon_v-\varepsilon_1$ relation. Here, only an isotropic consolidation test represented by the open circle with dot is performed by means of the ordinary stress controlled method, the other tests are performed by means of the strain controlled method using an automatically controlled apparatus. It is apparent from these figure that the proposed model explains the observed stress-strain behavior in various consolidation tests under triaxial compression and extension conditions.

In Figs. 19(a) and (b) arranged are the observed values in these various shear and consolidation tests under triaxial compression and extension conditions, in terms of the re-

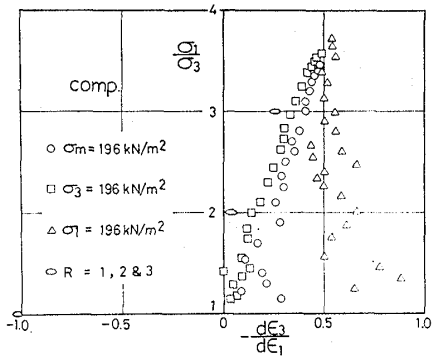

(a) triaxial compression

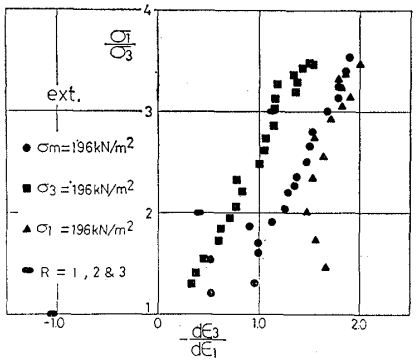

(b) triaxial extension

Fig. 19. Observed relation between principal stress ratio (σ_1/σ_3) and principal strain increment ratio ($-d\varepsilon_3/d\varepsilon_1$) in various shear and consolidation tests

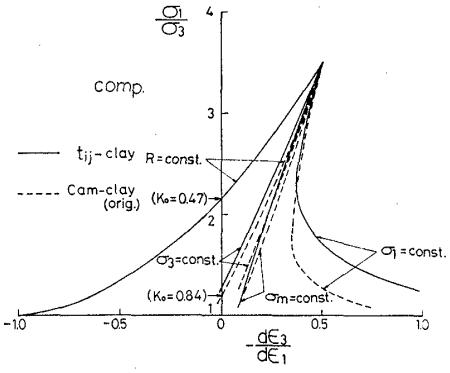

(a) triaxial compression

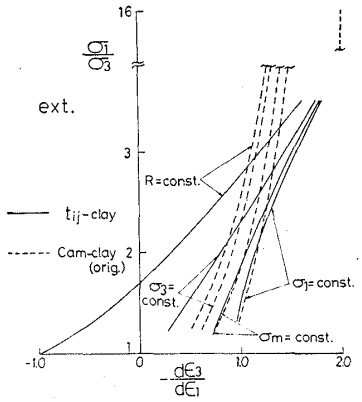

(b) triaxial extension

Fig. 20. Calculated relation between principal stress ratio (σ_1/σ_3) and principal strain increment ratio ($-d\varepsilon_3/d\varepsilon_1$) in various shear and consolidation tests

lation between σ_1/σ_3 and $-d\varepsilon_3/d\varepsilon_1$. Figs. 20 (a) and (b) show the corresponding analytical results by the proposed model(solid lines) and the Cam-clay model (broken lines). Camparing the observed values in Fig. 19 with the analytical results in Fig. 20, we can find that the proposed model can describe the dependence of the observed stress ratio-strain increment ratio relation on the stress paths under triaxial compression and extention conditions, though the Cam-clay model does not describe such a tendency of the observed values. Moreover, it is seen from Fig. 20(a) that the value of K_0 predicted by the proposed model is appropriate($K_0=0.47$), while the value by the Cam-clay model is too large ($K_0=0.84$) for a normally consolidated clay. To clarify the difference between these two model, the analytical stress ratio-plastic strain increment ratio relations are shown in Figs. 21(a) and (b) in terms of q/p vs. $-d\varepsilon_v^p/d\varepsilon_d^p$ by using the stress parameters and plastic strain increment parameters employed in the Cam-clay model(see Eqs. (8), (9), (15) and (16)). According to the Cam-clay model, all the plastic strain increments satisfy the same relation given by Eq. (14), regardless of the stress paths(e. g. $\sigma_m=$const., $\sigma_3=$const., $\sigma_1=$const. and $R=$const. paths). On the other hand, the plastic strain increment ratio based on the proposed model changes depending on the stress paths, since the plastic strain increment is given as the summation of $d\varepsilon_{ij}^{p(AF)}$ and $d\varepsilon_{ij}^{p(IC)}$. To be more precise, though the relations between stress ratio and plastic strain increment ratio are the same under the stress path of $dt_N \leqq 0$ such as $\sigma_m=$const. and $\sigma_1=$const. (since $d\varepsilon_{ij}^p = d\varepsilon_{ij}^{p(AF)}$), those are different under the stress

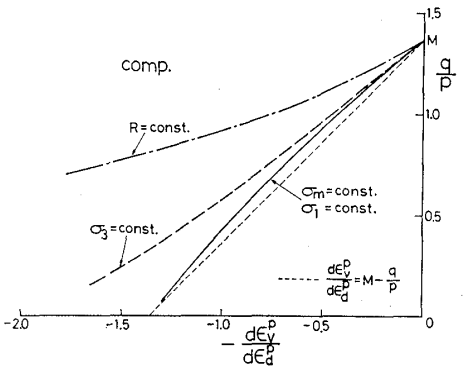

(a) triaxial compression

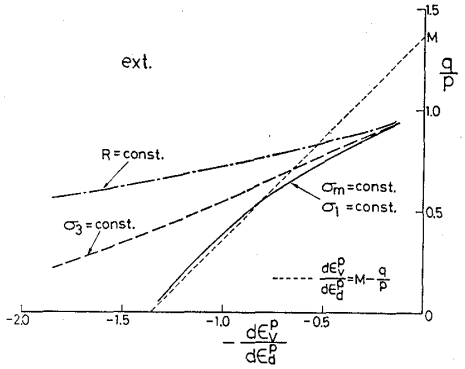

(b) triaxial extension

Fig. 21. Analytical relation between stress ratio (q/p) and plastic strain increment ratio ($-d\varepsilon_v^p/d\varepsilon_d^p$) by t_{ij}-clay model and original Cam-clay model

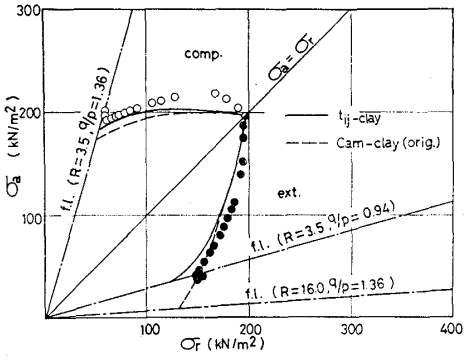

Fig. 22. Effective stress paths in undrained triaxial compression and extension tests

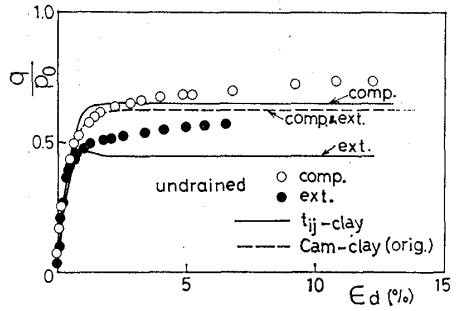

Fig. 23. Stress-strain relationship in undrained triaxial compression and extension tests

path of $dt_N>0$ such as σ_3=const. and R=const. (since $d\varepsilon_{ij}^p=d\varepsilon_{ij}^{p(AF)}+d\varepsilon_{ij}^{p(IC)}$). It is also seen in Figs. 21(a) and (b) that the relations between q/p and $d\varepsilon_v^p/d\varepsilon_d^p$ by the Cam-clay model are the same regardless not only of the stress paths but also of the stress conditions (e. g. triaxial compresion and extension conditions), but those by the proposed model are different. These differences in plastic strain increment ratio depending on the stress paths and stress conditions calculated by the proposed model incorporate with many experimental results reported(e. g. Lewin and Burland, 1970 ; Ohmaki, 1982). Now then, it is due to the influence of the elastic component that the Cam-clay model describes a little stress path dependency of total strain increment ratios in Fig. 20.

Fig. 22 shows the effective stress paths in undrained triaxial compression and extension tests, in terms of the relation between axial stress σ_a and radial stress σ_r. The open and solid dots represent the observed values, and the solid and broken curves represent the analytical results by the proposed model and the original Cam-clay model respectively. Here, though the failure lines in the proposed model and the Cam-clay model are the same (R=3.5, q/p=1.36) under triaxial compression condition, the failure line in the proposed model (R=3.5, q/p=0.94) is different from that in the Cam-clay model (R=16.0, q/p=1.36) under triaxial extension condition. Fig. 23 shows the analytical undrained stress-strain curves by the both models and the observed values. Here, $q=\sigma_1-\sigma_3$, $\varepsilon_d=(2/3)(\varepsilon_1-\varepsilon_3)$ and p_0 is the initial confining pressure(p_0=196 kN/m²). It is seen from Figs. 22 and 23 that though there is no significant difference between the analytical results by the both models under triaxial

compression condition, the proposed model can describe the differences of the undrained strength and the deformation behavior between triaxial compression and extension conditions, which are not represented by the Cam-clay model. Now, as is seen in e. g. Figs. 12, 13 and 15 described before, though the principal strains and the shear strains to failure predicted by the proposed model are infinite under triaxial compression condition, those are finite under such stress condition as triaxial extension and plane strain except for triaxial compression condition. This tendency is also shown in the observed values. Therefore, the undrained stress-strain curve after failure under triaxial extension by the proposed model in Fig. 23 is drawn as a perfect plastic material without further volume change.

Figs. 25(a) to (d) show the observed values (dots) and the analytical stress-strain curves by the proposed model under the various stress paths from point A to point G in Fig. 24(paths AEFG, ABFG, ACFG and ADFG), arranged with respect to the relations between σ_1/σ_3 and (ε_1 and ε_3) and relations between ε_1 and ε_v. Here, the stress conditions (σ_a, σ_r) of points A to F in Fig. 24 are as follows : A=(196, 196), B=(441, 441), C=(588, 588), D=(784, 784), E=(294, 147) and F=(882, 441) in kN/m². It is seen from these figures that the proposed model describes the observed stress-strain behavior of clay under the various stress paths combining shear and consolidation as well.

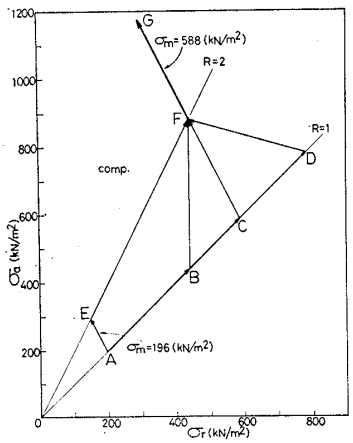

Fig. 24. Stress paths of triaxial compression tests (paths AEFG, ABFG, ACFG and ADFG) represented in (σ_a, σ_r) space

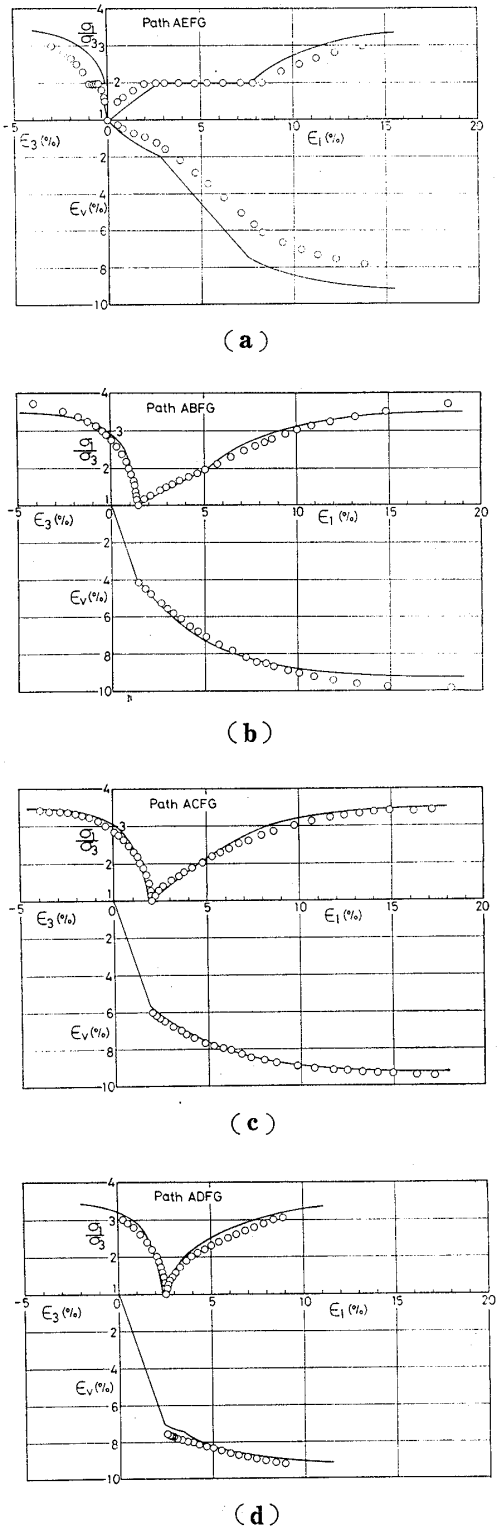

(a) (b) (c) (d)

Fig. 25. Stress-strain curves under various stress paths from points A to G in Fig. 24

CONCLUSIONS

The main results of this paper are summarized as follows :

(1) A simple and general elastoplastic constitutive model for clay is proposed that describes precisely the stress-strain behavior of clay under various stress paths in three-dimensional stresses. In this model, the influence of the intermediate principal stress are considered by using the mechanical quantity t_{ij} which is a generalization of the concept of SMP*, and the influence of the stress path by dividing the plastic strain increment into the component satisfying the associated flow rule in the t_{ij}-space and the component compressive isotropically. Furthermore, its soil parameters can be easily determined in the same way as the Cam-clay model, because only a yield function and a strain hardening parameter are used in the model.

(2) Various kinds of soil element tests of clay under triaxial compression, triaxial extension and plane strain conditions are analyzed using the proposed model. Then the validities of the the model are confirmed by comparing the analytical results with the observed values and the results calculated by the Cam-clay model. The proposed model explains precisely the observed stress-strain behavior in σ_3=const., σ_1=const., σ_m=const., σ_1/σ_3=const. and undrained tests under triaxial compression and extension conditions and predicts adequately the stress-strain behavior under plane strain condition.

Although in the present paper the validities of the proposed model are checked by the test results under triaxial compression and extension conditions only, the comparisons between the analytical results and the observed values under three different principal stresses conditions are shown in another paper(Nakai et al., 1986).

ACKNOWLEDGEMENTS

The authors wish to thank Prof. T. Yamauchi at Nagoya Institute of Technology for his helpful support and encouragement. They are also indebted to Messrs. K. Fujiwara, T. Haruki, N. Okuno, K. Tsuzuki and T. Asai for their experimental assistance and useful discussion. This study was done by the financial support of Grant-in-Aid for Encouragement of Young Scientist (No. 58750400 and No. 59750385) from the Ministry of Education, Science and Culture.

APPENDIX 1

The concrete derivations of the stress ratio X_f and plastic strain increment ratio Y_f at failure in Eqs. (22) and (23) are given below :

Under a triaxial compression condition($\sigma_1 > \sigma_2=\sigma_3$ and $d\varepsilon_1 > d\varepsilon_2=d\varepsilon_3$) the stress ratio, $X\equiv t_S/t_N$, and the plastic strain increment ratio, $Y\equiv d\varepsilon_{SMP}{}^{*p}/d\gamma_{SMP}{}^{*p}$, are expressed as follows from Eqs. (1), (7), (17) and (18) :

$$X\equiv\frac{t_S}{t_N}=\frac{\sqrt{2}}{3}\left(\sqrt{\frac{\sigma_1}{\sigma_3}}-\sqrt{\frac{\sigma_3}{\sigma_1}}\right) \tag{A1}$$

$$Y\equiv\frac{d\varepsilon_{SMP}{}^{*p}}{d\gamma_{SMP}{}^{*p}}=\frac{d\varepsilon_1{}^p a_1+2d\varepsilon_3{}^p a_3}{\sqrt{2}\,(d\varepsilon_1{}^p a_3-d\varepsilon_3{}^p a_1)}=\frac{1+2\sqrt{\frac{\sigma_1}{\sigma_3}}\cdot\left(\frac{d\varepsilon_3{}^p}{d\varepsilon_1{}^p}\right)}{\sqrt{2}\left\{\sqrt{\frac{\sigma_1}{\sigma_3}}-\left(\frac{d\varepsilon_3{}^p}{d\varepsilon_1{}^p}\right)\right\}} \tag{A2}$$

Since at the critical state, i. e. at failure, in triaxial compression the plastic volumetric strain increment $d\varepsilon_v{}^p$ is zero, the plastic principal strain increment ratio $d\varepsilon_3{}^p/d\varepsilon_1{}^p$ is

$$\frac{d\varepsilon_3{}^p}{d\varepsilon_1{}^p}=\frac{1}{2}\left(\frac{d\varepsilon_v{}^p}{d\varepsilon_1{}^p}-1\right)=-\frac{1}{2} \tag{A3}$$

Therefore, X_f and Y_f are expressed using the principal stress ratio at failure, $R_f\equiv(\sigma_1/\sigma_3)_{f(\text{comp.})}$, as follows

$$X_f=\frac{\sqrt{2}}{3}\left(\sqrt{R_f}-\sqrt{\frac{1}{R_f}}\right) \tag{22}$$

$$Y_f=\frac{1-\sqrt{R_f}}{\sqrt{2}\,(\sqrt{R_f}+0.5)} \tag{23}$$

APPENDIX 2

The concrete forms of the derivatives $\partial f/\partial t_{ij}$, $\partial f/\partial\varepsilon_v{}^p$, $\partial\varepsilon_v{}^p/\partial\varepsilon_{ij}{}^p$ and $\partial f/\partial\sigma_{ij}$ are expressed as follows :

(i) Since the yield function f is given as

a function of t_N and X, and t_{ij} is a symmetrical tensor whose principal axes coincide with those of σ_{ij} in direction, $\partial f/\partial t_{ij}$ is calculated as

$$\frac{\partial f}{\partial t_{ij}}=\left(\frac{\partial f}{\partial t_N}\cdot\frac{\partial t_N}{\partial t_k}+\frac{\partial f}{\partial X}\cdot\frac{\partial X}{\partial t_k}\right)\cdot\frac{\partial t_k}{\partial t_{ij}}$$
$$=\left(\frac{\partial f}{\partial t_N}\cdot\frac{\partial t_N}{\partial t_k}+\frac{\partial f}{\partial X}\cdot\frac{\partial X}{\partial t_k}\right)\cdot\frac{\partial \sigma_k}{\partial \sigma_{ij}} \quad (A4)$$

Here, from Eq. (29),

$$\frac{\partial f}{\partial t_N}=\frac{\lambda-\kappa}{1+e_0}\cdot\frac{1}{t_N} \quad (A5)$$

$$\frac{\partial f}{\partial X}=\frac{\lambda-\kappa}{1+e_0}\cdot\frac{\alpha}{M^*-(1-\alpha)\cdot X} \quad (A6)$$

and from Eqs. $(5)_1$ and $(6)_1$,

$$\frac{\partial t_N}{\partial t_1}=a_1,\quad \frac{\partial t_N}{\partial t_2}=a_2,\quad \frac{\partial t_N}{\partial t_3}=a_3 \quad (A7)$$

$$\frac{\partial X}{\partial t_1}=\frac{\partial\left(\frac{t_S}{t_N}\right)}{\partial t_1}=\frac{\partial t_S}{\partial t_1}\cdot\frac{1}{t_N}-\frac{\partial t_N}{\partial t_1}\cdot\frac{X}{t_N}$$
$$=\frac{(t_1a_2-t_2a_1)a_2+(t_1a_3-t_3a_1)a_3}{t_S}\cdot\frac{1}{t_N}$$
$$-a_1\cdot\frac{X}{t_N} \quad (A8)$$

$\partial X/\partial t_2$ and $\partial X/\partial t_3$ are also given in the same way as Eq. (A 8). Furthermore, since the principal axes of symmetrical tensors t_{ij} and σ_{ij} coincide in direction, $\partial t_k/\partial t_{ij}$ ($k=1, 2$ and 3) are equal to $\partial\sigma_k/\partial\sigma_{ij}$ and are expressed as functions of σ_{ij}. For reference, the forms of $\partial t_k/\partial t_{ij}$ ($k=1, 2$ and 3) in the case of $\sigma_{13}=\sigma_{23}=0$ such as plane strain and axisymmetric conditions are shown in Appendix 1 of the previous paper(Nakai and Mihara, 1984).

(ii) From Eq. (29),

$$\frac{\partial f}{\partial \varepsilon_v{}^p}=-1 \quad (A9)$$

(iii) Since $\varepsilon_v{}^p=\delta_{ij}\cdot\varepsilon_{ij}{}^p$,

$$\frac{\partial \varepsilon_v{}^p}{\partial \varepsilon_{ij}{}^p}=\delta_{ij} \quad (A10)$$

(iv) Since the terms t_N and X in the yield function of Eq. (29) are also given by Eqs $(5)_2$ and $(6)_2$, $\partial f/\partial\sigma_{ij}$ is calculated as

$$\frac{\partial f}{\partial \sigma_{ij}}=\frac{\partial f}{\partial t_N}\cdot\frac{\partial t_N}{\partial \sigma_{ij}}+\frac{\partial f}{\partial X}\cdot\frac{\partial X}{\partial \sigma_{ij}} \quad (A11)$$

where $\partial f/\partial t_N$ and $\partial f/\partial X$ are given by Eqs. (A 5) and (A 6), and $\partial X/\partial\sigma_{ij}$ are expressed as

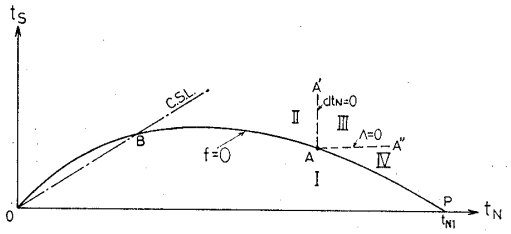

Fig. A 1. Proposed yield surface f in (t_N, t_S) space and four regions where developments of strain are different when stress condition moves from point A

$$\frac{\partial t_N}{\partial \sigma_{ij}}=\frac{\partial\left(3\frac{J_3}{J_2}\right)}{\partial \sigma_{ij}} \quad (A12)$$

$$\frac{\partial X}{\partial \sigma_{ij}}=\frac{\partial\left(\sqrt{\frac{J_1J_2-9J_3}{9J_3}}\right)}{\partial \sigma_{ij}} \quad (A13)$$

APPENDIX 3

The method to formulate the model is shown here when Λ of Eq (32) is zero or negative :

From Eq. (32), the condition that Λ is not positive is expressed as

$$\frac{dX}{dt_N}\leqq-\frac{\frac{\partial f}{\partial t_N}-\frac{1}{t_{N_1}}}{\frac{\partial f}{\partial X}} \quad (A14)$$

where $\partial f/\partial t_N$, $\partial f/\partial X$ and t_{N1} are given by Eqs. (A 5), (A 6) and (37), respectively, and on deriving Eq. (A 14) from Eq. (32) the relations of Eqs. (36), (A 9), (A 10) are utilized. If we show the condition of $f=0$, $df>0$ and $\Lambda\leqq 0$ in the (t_N, t_S) space, it is indicated by the region IV in Fig. A 1. Here, it is assumed that only the plastic strain increment compressive isotropically occurs in region IV

$$d\varepsilon_{ij}{}^p=\Lambda'\cdot\frac{\delta_{ij}}{3} \quad (A15)$$

where Λ' is given as follows from the condition of consistency of Eq. (30), and Eq. (A 15),

$$\Lambda'=-\frac{\frac{\partial f}{\partial \sigma_{ij}}d\sigma_{ij}}{\frac{\partial f}{\partial \varepsilon_v{}^p}\cdot\frac{\partial \varepsilon_v{}^p}{\partial \varepsilon_{kl}{}^p}\cdot\frac{\delta_{kl}}{3}}=\frac{\partial f}{\partial \sigma_{ij}}d\sigma_{ij} \quad (A16)$$

REFERENCES

1) Hambly, E. C. (1972) : "Plane strain behaviour of remoulded normally consolidated kaolin," Géotechnique, Vol. 22, No. 2, pp. 301-317.
2) Karube, D. (1975) : "Nonstandard triaxial testing method and its problems," Proc., 20 th Symposium on Soil Engineering, JSSMFE, pp. 45-60 (in Japanese).
3) Lade, P. V. (1979) : "Stress-strain theory for normally consolidated clay," Proc., 3 rd Int. Conf. on Numerical Method in Geomechanics, Vol. 4, pp. 1325-1337.
4) Lade, P. V. and Musante, H. M. (1978) : "Three-dimensional behavior of remoulded clay," Proc. ASCE, Vol. 104, No. GT 2, pp. 193-209.
5) Lewin, P. I. and Burland, J. B. (1970) : "Stress-probe experiments on saturated normally consolidated clay," Géotechnique, Vol. 20, No. 1, pp. 38-56.
6) Matsuoka, H. and Nakai, T. (1974) : "Stress-deformation and strength characteristics of soil under three different principal stresses," Proc., JSCE, No. 232, pp. 59-70.
7) Matsuoka, H. and Nakai, T. (1977) : "Stress-strain relationship of soil based on the SMP," Proc., Specialty Session 9, 9 th ICSMFE, pp. 153-162.
8) Nakai, T. (1985) : "Finite element computations for active and passive earth pressure problems of retaining wall," Soils and Foundations, Vol. 25, No. 3, pp. 98-112.
9) Nakai, T. and Matsuoka, H. (1980) : "A unified law for soil shear behavior under three-dimensional stress condition," Proc., JSCE, No. 303, pp. 65-77 (in Japanese).
10) Nakai, T. and Matsuoka, H. (1981) : "A unified law for soil deformation behavior under various stress paths," Proc. JSCE, No. 306, pp. 23-34 (in Japanese).
11) Nakai, T. and Matsuoka, H. (1983 a) : "Shear behaviors of sand and clay under three-dimensional stress condition," Soils and Foundations, Vol. 23, No. 4, pp. 87-106.
12) Nakai, T. and Matsuoka, H. (1983 b) : "Constitutive equation for soils based on the extended concept of "Spatial Mobilized Plane" and its application to finite element analysis," Soils and Foundations, Vol. 23, No. 4, pp. 87-105.
13) Nakai, T., Matsuoka, H., Okuno, N. and Tsuzuki, K. (1986) : "True triaxial tests on normally consolidated clay and analysis of the observed shear behavior using elastoplastic constitutive models," Soils and Foundations, (accepted for publication).
14) Nakai, T. and Mihara, Y. (1984) : "A new mechanical quantity for soils and its application to elastoplastic constitutive models," Soils and Foundations, Vol. 24, No. 2, pp. 82-94.
15) Nakai, T., Shibata, T. and Matsuoka, H. (1982) : "Finite element analysis of soil foundation below an embankment," Proc., 4 th Int. Conf. on Numerical Methods in Geomechanics, Vol. 2, pp. 707-715.
16) Ohmaki, S. (1979) : "A mechanical model for the stress-strain behaviour of normally consolidated cohesive soil," Soils and Foundations, Vol. 19, No. 3, pp. 29-44.
17) Ohmaki, S. (1982) : "Stress-strain behaviour of anisotropically, normally consolidated cohesive soil," Proc., Int. Symposium on Numerical Models in Geomechanics, pp. 260-269.
18) Ohta, H. (1971) : "Analysis of deformation of soils based on theory of plasticity and its application to settlement of embankments," Dr. Eng. Thesis, Kyoto Univ.
19) Pender, M. J. (1977) : "A unified model for soil stress-strain behavior," Proc., Specialty Session 9, 9 th ICSMFE, pp. 213-222.
20) Roscoe, K. H. and Burland, J. B. (1968) : "On the generalized stress-strain behaviour of wet clay," Engineering Plasticity Cambridge Univ. Press, pp. 535-609.
21) Roscoe, K. H., Schofield, A. N. and Thurairajah, A. (1963) : "Yieling of clays in states wetter than critical," Géotechnique, Vol. 13, No. 3, pp. 211-240.
22) Schofield, A. N. and Wroth, C. P. (1968) : Critical State Soil Mechanics, McGraw-Hill, London.
23) Vaid, Y. P. and Campanella, R. G. (1974) : "Triaxial and plane strain behavior of natural clay," Proc., ASCE, Vol. 100, No. GT 3, pp. 207-224.
24) Yong, R. N. and Mckyes, E. (1971) : "Yield and failure of clay under triaxial stresses," Proc., ASCE, Vol. 97, No. SM 1, pp. 159-176.